Economic Geology, v. XXX, no. XX, pp. X–X

SCIENTIFIC COMMUNICATIONS

MINERAL PARAGENESIS OF EARLY BIOTITE VEINS AT THE KUH-E JANJA Cu-Au PORPHYRY DEPOSIT, SOUTHEASTERN IRAN: IMPORTANCE OF MICROTEXTURAL OBSERVATIONS IN STUDIES CONSTRAINING THE RELATIVE TIMING OF HYPOGENE Cu MINERALIZATION

Majid Soleymani,[1] Thomas Monecke,[2,†] T. James Reynolds,[2,3] and Shojaeddin Niroomand[1]

[1]*School of Geology, College of Science, University of Tehran, Tehran P94W+294, Iran*

[2]*Center to Advance the Science of Exploration to Reclamation in Mining, Department of Geology and Geological Engineering, Colorado School of Mines, 1516 Illinois Street, Golden, Colorado 80401, USA*

[3]*FLUID INC., 1401 Wewatta Street #PH3, Denver, Colorado 80202, USA*

Abstract

Veins consisting primarily of biotite are the earliest stockwork vein type recognized at the Kuh-e Janja Cu-Au porphyry deposit in southeastern Iran. These early biotite veins may contain quartz and minor amounts of sulfide minerals such as chalcopyrite and pyrite. Observations at the hand-specimen scale do not provide reliable constraints on the paragenetic relationships, as the early biotite veins have been repeatedly overprinted during the evolution of the magmatic-hydrothermal system. Microscopic investigations show that the sulfide minerals in the early biotite veins are texturally late, providing evidence that sulfide deposition did not occur at the high temperatures of biotite formation and potassic alteration of the host rocks. Chalcopyrite primarily occurs along hairline fractures that crosscut or refracture the earlier biotite veins. Biotite in contact with the chalcopyrite can be apparently unaltered or is replaced by chlorite, depending on the degree of wall-rock buffering of the magmatic-hydrothermal fluids that caused hypogene Cu mineralization. The findings add to the growing body of evidence that Cu mineralization in this deposit type occurs at temperatures close to the transition from ductile to brittle conditions (<450°C) following a drop in the pressure regime from lithostatic to hydrostatic conditions.

Introduction

Porphyry deposits are the world's most important source of Cu and Mo, with precious metals Au and Ag commonly recovered as by-products (Sillitoe, 2010). Hypogene ores in these deposits constitute large, low-grade stockwork and disseminated sulfide zones that are spatially associated with plutonic stocks and dike swarms emplaced at shallow (≤1–10 km) crustal depths (Lowell and Guilbert, 1970; Gustafson and Hunt, 1975; Titley and Beane, 1981; Seedorff et al., 2005; Sillitoe, 2010). The stockwork zones are composed of a characteristic sequence of crosscutting vein generations that can be distinguished based on morphology, vein mineralogy, and associated alteration (Nielsen, 1968; Gustafson and Hunt, 1975; Clark, 1993; Gustafson and Quiroga, 1995; Arancibia and Clark, 1996; Muntean and Einaudi, 2000; Monecke et al., 2018, 2019).

In many Cu-Au and Cu-Mo porphyry deposits, the earliest vein types recognized contain biotite. The biotite forms millimeter-wide veins, referred to as early biotite (EB) veins (Gustafson and Quiroga, 1995; Chang et al., 2017; Gregory, 2017; Ouyang et al., 2021). In some deposits, the early biotite forms the matrix of biotite-rich breccias (Brimhall, 1977; Gustafson and Quiroga, 1995). Biotite also occurs as green to dark-brown halos around hairline fractures and early veins, referred to as early dark micaceous (EDM) alteration envelopes (Meyer, 1965; Atkinson et al., 1996; Rusk et al., 2008; Proffett, 2009; Redmond and Einaudi, 2010; Rees et al., 2015; Cernuschi et al., 2018, 2023). The mineral paragenesis of the EB veins and EDM alteration envelopes has been a matter of debate for over a decade (Landtwing et al., 2010). In many deposits, the biotite in veins and alteration envelopes contains magnetite (Brimhall, 1977; Gustafson and Quiroga, 1995; Rusk et al., 2008; Maydagán et al., 2015). At Bingham Canyon, Utah (Redmond and Einaudi, 2010), Butte, Montana (Meyer, 1965; Brimhall, 1977; Rusk et al., 2008), El Salvador, Chile (Gustafson and Quiroga, 1995), and Haquira East, Peru (Cernuschi et al., 2018, 2023), the early biotite occurs with quartz and anhydrite. In addition, K-feldspar, sericite, and/or andalusite may be present (Meyer, 1965; Brimhall, 1977; Gustafson and Quiroga, 1995; Rusk et al., 2008; Redmond and Einaudi, 2010).

An important question relates to the presence of chalcopyrite and pyrite in the biotite-rich veins and alteration envelopes. Previous authors have taken the presence of these sulfide minerals to suggest that hypogene Cu mineralization in some porphyry deposits occurs early in the evolution of the magmatic-hydrothermal systems at temperatures as high as ~500° to 650°C (Rusk et al., 2008; Redmond and Einaudi, 2010; Cernuschi et al., 2018, 2023). However, other workers showed that hypogene Cu mineralization is associated with the formation of veins primarily composed of sulfides at temperatures of <450°C and therefore postdates the high-tem-

[†]Corresponding author: e-mail, tmonecke@mines.edu

ISSN 0361-0128; doi:10.5382/econgeo.5082; 10 p.

Submitted: June 7, 2023 / Accepted: January 22, 2024

perature vein types in porphyry deposits (Landtwing et al., 2010; Stefanova et al., 2014; Monecke et al., 2018, 2023; Sun et al., 2021; Tsuruoka et al., 2021; Schirra et al., 2022). Resolving the conditions at which hypogene Cu mineralization is formed in porphyry deposits is key to understanding this deposit type and has important implications to exploration.

This contribution focuses on the description of textural relationships in EB veins from the Kuh-e Janja Cu-Au porphyry deposit in southeastern Iran. At Kuh-e Janja, biotite-rich veins are mostly barren, although some veins contain chalcopyrite and pyrite. Microtextural observations reveal that sulfide minerals present in the EB veins and alteration envelopes sometimes clearly crosscut the biotite and formed during a later hydrothermal overprint within the EB veins. The findings at Kuh-e Janja suggest that the paragenetic relationships of early biotite-rich veins cannot be simply constrained by macroscopic observations, as clear evidence for the late overprint is not commonly identifiable at the hand-specimen scale.

Regional Geology

The Kuh-e Janja Cu-Au porphyry deposit is located 60 km southeast of Nehbandan in the Sistan and Baluchestan province, southeastern Iran (Fig. 1A). The deposit is situated within the Eastern Iranian orogen, which is a N-trending 900-km-long mountainous belt along the border between Iran, Afghanistan, and Pakistan (Stöcklin, 1968). The Eastern Iranian orogen formed as the result of northeastward-directed subduction of a Sistan ocean basin and middle Eocene collision of the Lut microcontinent in the west and the Afghan microcontinent in the east (Camp and Griffis, 1982; Tirrul et al., 1983; Fotoohi Rad et al., 2005; Saccani et al., 2010; Angiboust et al., 2013; Bonnet et al., 2018).

The rocks in the Eastern Iranian orogen are divided into three main geologic elements (Fig. 1A). This includes the Ratuk complex in the east and the Neh complex in the west, which are interpreted to represent the former accretionary prism. Both complexes contain a wide variety of rock types, including Late Cretaceous ophiolite and mélange as well as Late Cretaceous to Eocene phyllite. Late Cretaceous to Paleogene marine sedimentary rocks deposited in the Sefidabeh fore-arc basin onlap both complexes, although present contacts are generally tectonic. In contrast to the highly tectonized rocks of the Ratuk and Neh complexes, the sedimentary rocks in the Sefidabeh basin exhibit a coherent stratigraphy that can be traced across the belt (Tirrul et al., 1983). The Sefidabeh basin contains a volumetrically small succession of calc-alkaline volcanic rocks (Fig. 1A), which are interpreted to be subduction related (Camp and Griffis, 1982). Typical arc-volcanic successions are not recognized in the Eastern Iranian orogen (Camp and Griffis, 1982).

The Kuh-e Janja Cu-Au porphyry deposit is located in the northwestern part of the Zahedan-Nehbandan magmatic belt, which comprises major Oligocene to Miocene igneous centers stretching ~200 km from the city of Zahedan to the city of Nehbandan in the northwest (Fig. 1A; Camp and Griffis, 1982). Intrusions range from calc-alkaline to shoshonitic in character and are mostly intermediate to felsic in compositions. Several postsubduction porphyry deposits occur in the belt, including Kuh-e Janja (K-Ar on hornblende: 16.5 ± 2.0 Ma; Camp and Griffis, 1982), Kuh-e Lar (Re-Os on molybdenite: 31.95 ± 0.11 and 29.72 ± 0.11 Ma; Boomeri et al., 2019), and Kuh-e Seyasteragi (K-Ar on hornblende: 19.2 ± 1.4 Ma; Camp and Griffis, 1982).

Deposit Geology

The Kuh-e Janja Cu-Au porphyry deposit has been explored by the Iran Minerals Production and Supply Company since 2016. The economic potential of the deposit has been tested by 66 diamond drill holes for a total of ~50 km of drilling. Preliminary assessment indicates that Kuh-e Janja comprises a resource of 502.2 million tons (Mt) of ore grading 0.27% Cu and 0.24 g/t Au.

Porphyry mineralization at Kuh-e Janja is hosted by an intrusive complex that was emplaced into folded Late Cretaceous to Paleocene flysch successions of the Sefidabeh fore-arc basin (Fig. 1B). The intrusive complex comprises two premineralization intrusive phases, namely a diorite-granodiorite intrusion that has a calc-alkaline affinity and a darker dioritic to gabbroic intrusion, which does not crop out on surface. Both intrusions are crosscut by postmineralization hornblende diorite and diorite-gabbro dikes that have an east to northeastern trend. The contacts between the intrusive complex and the flysch host rocks are marked by a zone of hornfels or skarn that is up to 400 m in width (Fig. 1B). The hornfels is less susceptible to erosion than the intrusive rocks, forming a series of rugged peaks. The top of the orebody is eroded, and the intrusive complex is largely covered by Quaternary alluvial terraces (Fig. 1B).

At Kuh-e Janja, ore zones are confined to areas of intense stockwork veining and abundant disseminated sulfides located at about 100 m above sea level (Fig. 2). The mineralized zone is open to depth, as only a few deep exploration drill holes exist. Based on the existing drilling, the highest Cu concentrations occur in the southern part of the orebody. The highest Au concentrations are present in the central part of the deposit above 250 m above sea level (Fig. 2). The hypogene Cu-Au mineralization at Kuh-e Janja has been overprinted by supergene oxidation, which resulted in the widespread replacement of chalcopyrite by chalcocite and covellite (Elyaspour, 2010; Soleymani et al., 2020).

Following the nomenclature of Gustafson and Hunt (1975) and Monecke et al. (2018, 2019), several distinct stockwork vein types have been identified in drill core at the Kuh-e Janja Cu-Au porphyry deposit. Texturally early are EB veins that consist primarily of biotite, although minor amounts of anhydrite, magnetite, and quartz are commonly present. The most abundant vein type at Kuh-e Janja is A veins, which are several millimeters to centimeters in thickness and have irregular to planar walls. The quartz in the A veins is grayish in color and vitreous. The A veins are surrounded by extensive potassic alteration, which is typified by abundant K-feldspar and shreddy biotite. Replacement of host-rock biotite and hornblende phenocrysts by shreddy biotite is common. In addition to A veins, AB veins occur in host rocks affected by potassic alteration. The AB veins are characterized by euhedral quartz crystals that are perpendicular to the vein walls or in vugs. Molybdenite occurs as ribbons in recrystallized quartz in the AB veins or as an infill in open spaces between the euhedral quartz crystals. The AB veins crosscut potassic-altered rock, suggesting that the veins formed under conditions of biotite

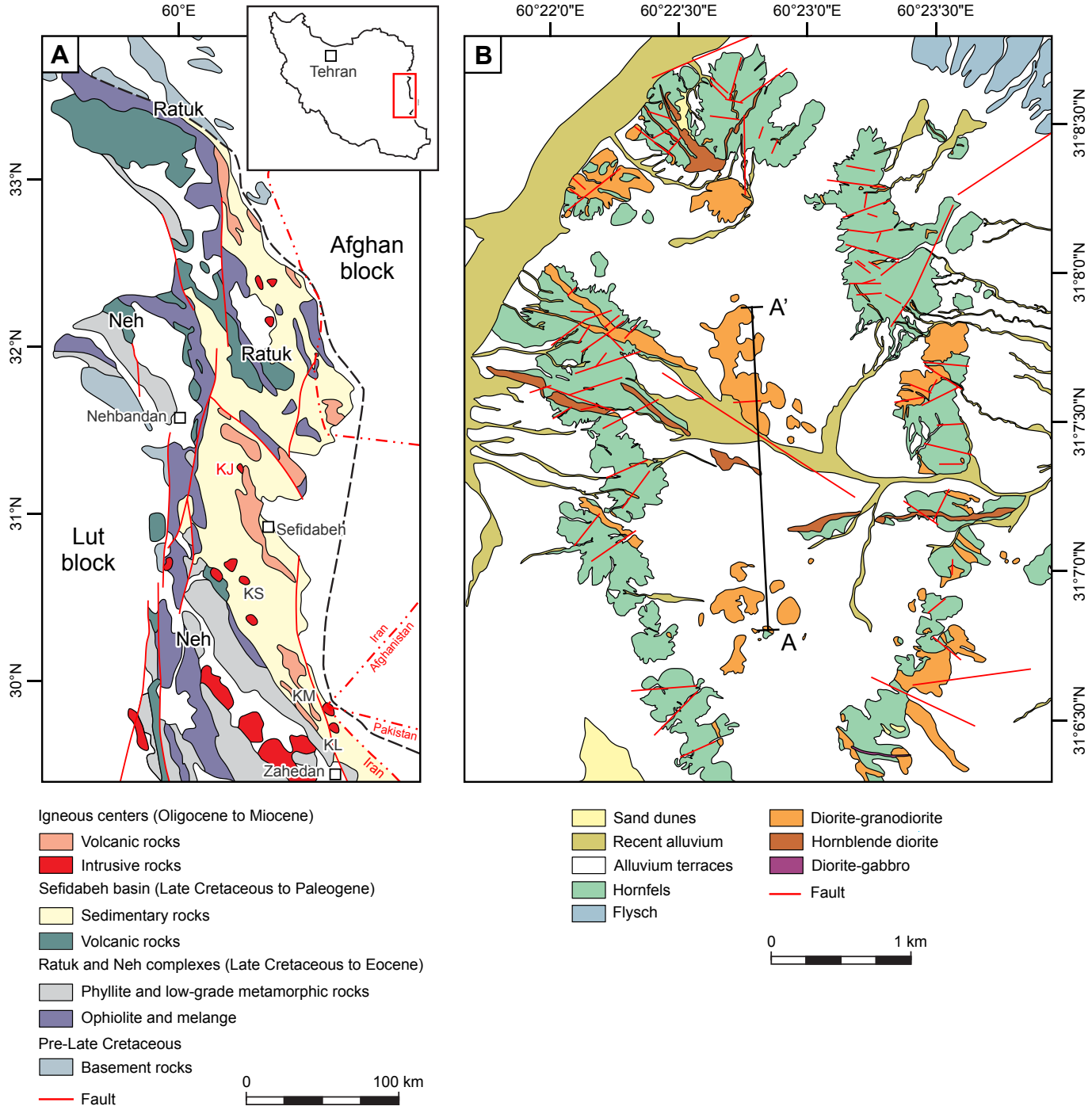

Fig. 1. Geologic setting of the Kuh-e Janja Cu-Au porphyry deposit. A. Map of the Eastern Iranian orogen and locations of porphyry deposits of the Zahedan-Nehbandan magmatic belt (modified from Camp and Griffis, 1982; Tirrul et al., 1983; Boomeri et al., 2020). B. Map of the deposit area showing the distribution of intrusive rocks that have been emplaced in flysch host rocks. The contact zone is marked by a zone of hornfels (modified from Parsolang Engineering Consultant Company, unpub. report, 2016, Final report of the preliminary exploration phase of the Kuh-e Janja prospect area, 176 p.). Porphyry deposits: KJ = Kuh-e Janja, KL = Kuh-e Lar, KM = Kuh-e Malek Siah, KS = Kuh-e Seyasteragi.

stability. Zones of high Cu grades at Kuh-e Janja are typified by abundant C veins, which are hairline fractures coated by chalcopyrite and pyrite. Minor chlorite is present in the hairline fractures and narrow alteration envelopes. However, in many cases the hairline fractures with sulfide coatings run along earlier stockwork veins. In these cases, chlorite alteration envelopes are commonly difficult to identify in hand specimens or with a hand lens. Late D veins consisting of vari-

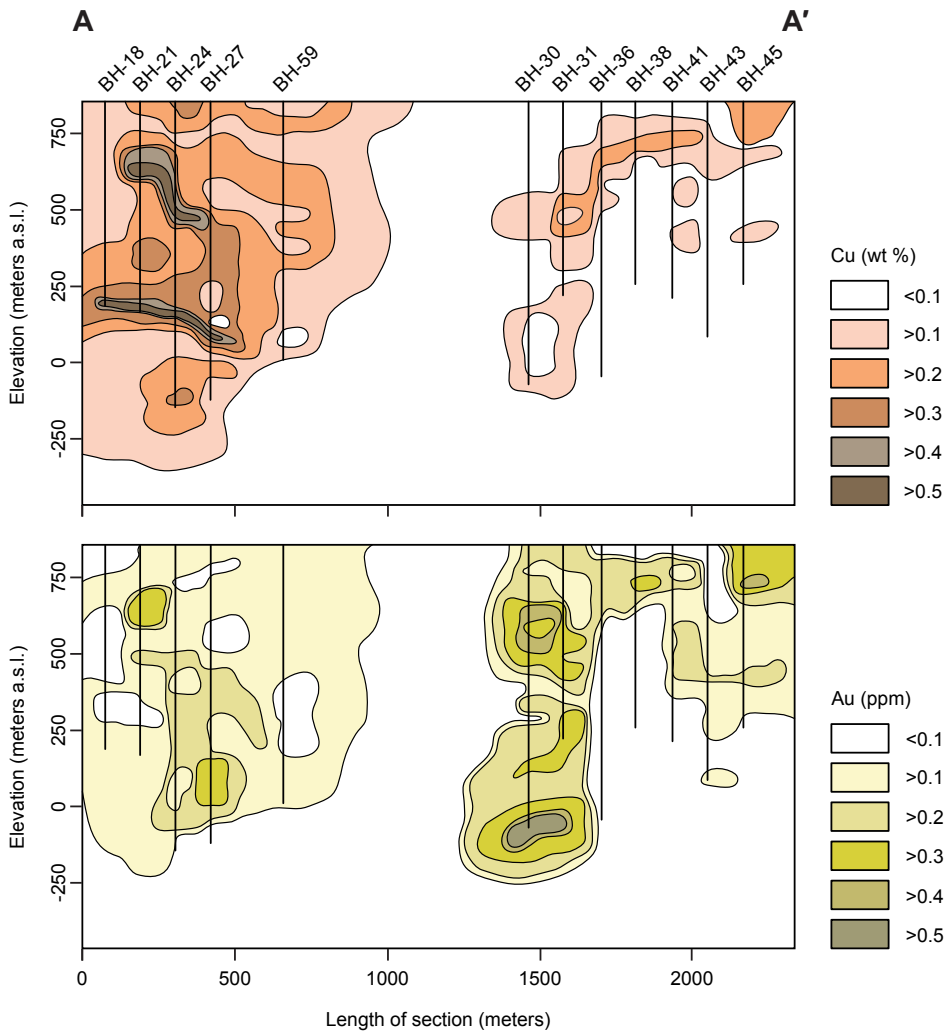

Fig. 2. Distribution of Cu and Au grades along a north-south section through the Kuh-e Janja Cu-Au porphyry deposit. The location of the section is shown in Figure 1B. Data provided by the Iran Minerals Production and Supply Company (unpub. report, 2022). Abbreviation: a.s.l. = above sea level.

able proportions of pyrite and quartz, associated with intense and texturally destructive sericite alteration of the host rocks, are abundant throughout the deposit. Rare polymetallic E veins containing sphalerite, galena, and minor chalcopyrite also occur. Outside of the immediate deposit area, the intrusive rocks and the sedimentary host rocks have been affected by propylitic alteration characterized by epidote, chlorite, pyrite, and calcite.

Results

Logging of selected exploration drill core showed that EB veins at Kuh-e Janja typically are planar hairline fractures filled by biotite (Fig. 3A). In some cases, the hairline fractures are surrounded by EDM alteration halos up to 5 mm in width (Fig. 3B). The amount of biotite in the EB veins is variable, with some of the hairline fractures being filled by biotite over strike lengths of several centimeters while others only contain patchy biotite along the fractures. Some of the EB veins are partially filled by vitreous gray quartz or show gradations from biotite to rich in quartz (Fig. 3A, C). Most of the veins are barren and lack sulfide minerals, although grains of pyrite and chalcopyrite can be present (Fig. 3A, C). The hairline fractures are commonly surrounded by potassic alteration halos that are rich in K-feldspar and typically pink in color (Fig. 3A). EDM alteration envelopes frequently grade outward into alteration halos containing abundant K-feldspar (Fig. 3B).

Core logging also confirmed that the EB veins formed early in the evolution of the magmatic-hydrothermal system at Kuh-e Janja. The hairline fractures containing abundant biotite and the EDM alteration halos are consistently crosscut by A veins consisting of vitreous gray quartz, or grade into fractures filled with quartz that is texturally indistinguishable from quartz forming A veins (Fig. 3B, C). Rare examples of AB veins crosscutting or reopening the EB veins have been observed. The EB veins are also crosscut or refractured by C veins that are primarily composed of chalcopyrite and pyrite. The C veins are surrounded by pale-green to brown alteration halos containing chlorite (Fig. 3D).

Representative EB veins were selected for thin-section preparation to unravel textural relationships at the microscale.

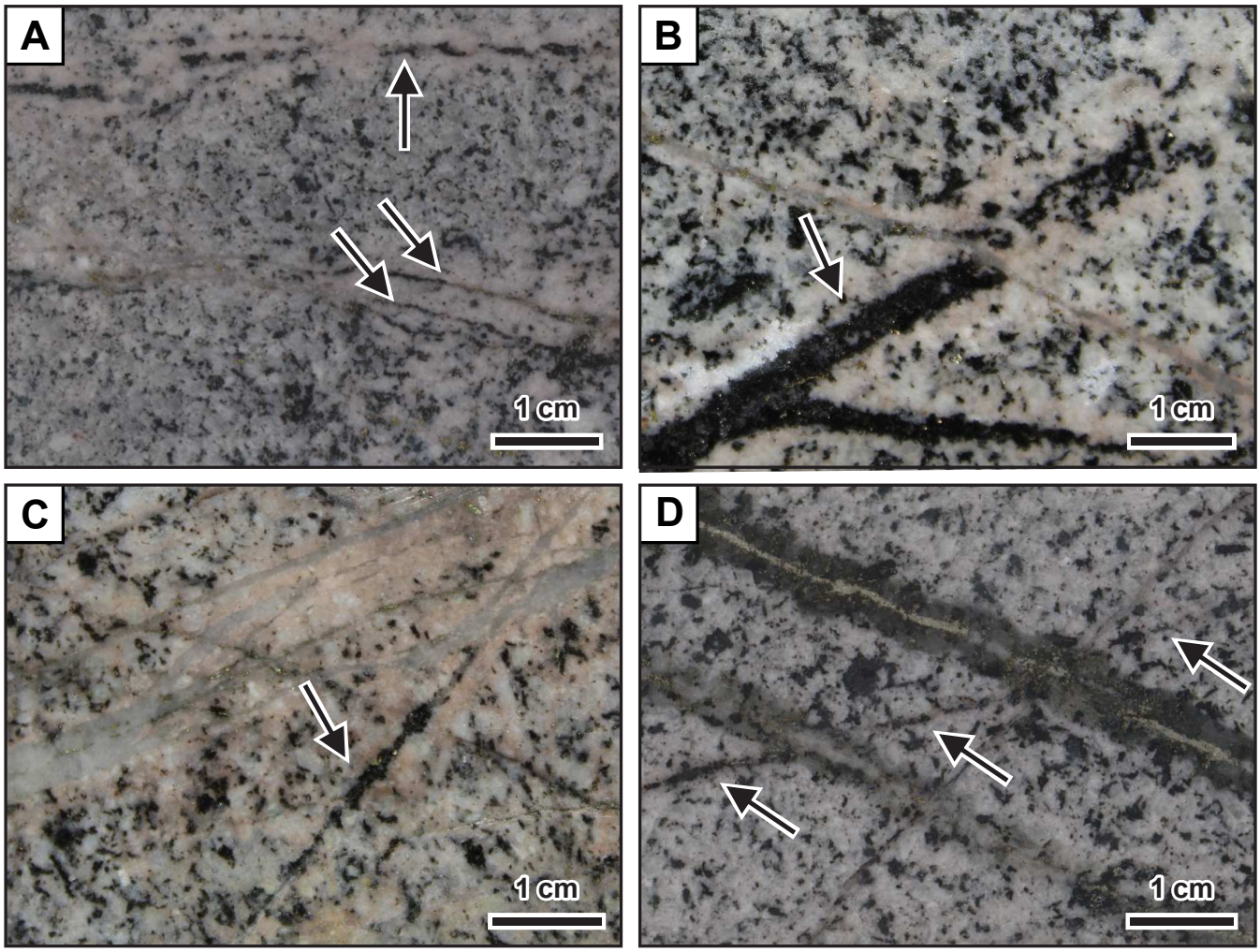

Fig. 3. Core samples showing crosscutting relationships between early biotite (EB) veins and later stockwork vein types at the Kuh-e Janja Cu-Au porphyry deposit. A. Hairline EB veins (arrows) surrounded by potassic alteration envelopes that are distinctly pink in color. The amount of biotite along the hairline fractures is variable. Quartz and chalcopyrite are present along the same fractures. Sample BH-68-779. B. Early dark micaceous alteration halo surrounding a hairline fracture. The alteration halo is crosscut and offset by a narrow A vein. Sample BH-68-795. C. EB vein (arrow) that changes compositionally along the hairline fracture. In the lower part of the core image, the hairline fracture is primarily filled by biotite and contains minor chalcopyrite. In the upper part of the image, the same hairline fracture is dominated by quartz. The hairline fracture is crosscut by several A veins. Sample BH-68-586. D. Hairline EB vein (arrows) that is crosscut and offset by a C vein containing abundant pyrite and some chalcopyrite. The C vein is surrounded by a pale-green to brown alteration envelope. Thin-section inspection shows that this alteration halo consists primarily of dark chlorite. Sample BH-68-686.

Optical microscopy confirmed that many of the EB veins contain anhydrite, magnetite, and/or quartz (Fig. 4A-C). Optical cathodoluminescence (CL) microscopy using a HC5-LM hot cathode CL microscope by Lumic Special Microscopes, Germany, was conducted to further study the quartz and anhydrite in the EB veins, with the instrument operated at 14 kV and a current density of ~10 µA mm^{-2} (Neuser, 1995). The quartz shows a stable blue CL emission, which is characteristic of high-temperature quartz in porphyry deposits (Monecke et al., 2018, 2023; Sun et al., 2021; Tsuruoka et al., 2021). The quartz forms anhedral grains that lack primary growth zoning. Anhydrite in the EB veins is brownish red in color and exhibits complex zoning patterns (Fig. 4D). The textural relationships observed do not conclusively constrain the timing of anhydrite, magnetite, and quartz formation. All three minerals could have precipitated with the biotite in the EB veins or may have been deposited during a later, high-temperature overprint of the EB veins.

Careful petrographic investigations were conducted to unravel the paragenetic relationships between the biotite and the hypogene Cu sulfides. In most cases, where chalcopyrite was observed in EB veins in drill core, the EB veins appear to have been refractured by a C vein that runs parallel to the biotite vein. However, EB veins are also crosscut by thin C veins at an angle providing unequivocal textural evidence for a paragenetically late introduction of the hypogene Cu sulfides (Fig. 5A). In the case of narrow C veins, the chalcopyrite forming these veins frequently dissects some of the larger

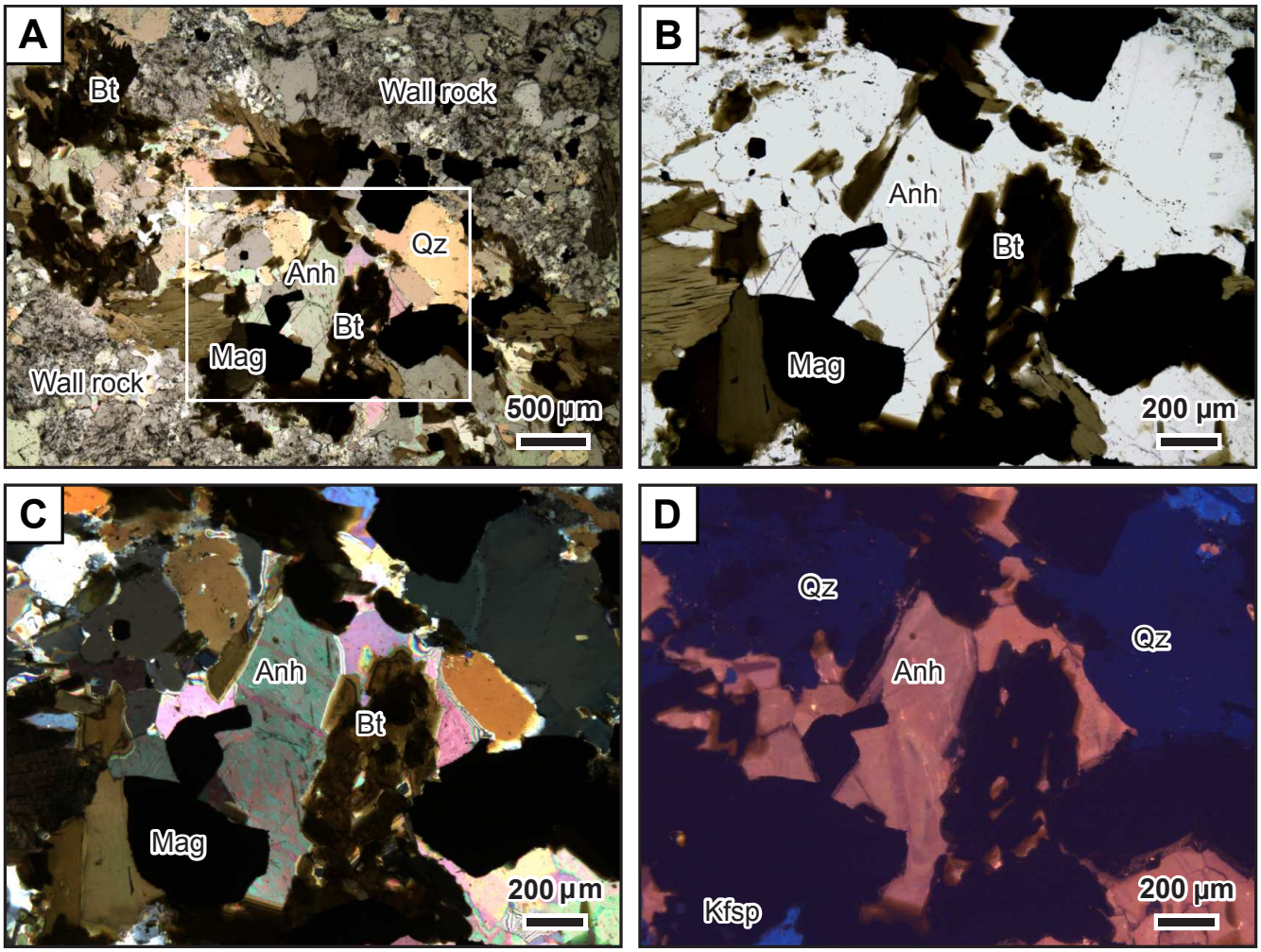

Fig. 4. Textural relationships in early biotite (EB) veins at the Kuh-e Janja Cu-Au porphyry deposit. A. EB vein containing anhydrite, magnetite, and quartz. Crossed-polarized light image. The rectangle shows the location of the high-magnification images in Figure 4B-D. The textural relationships are inconclusive and do not allow determination of the timing relationship between the different minerals. It is possible that the biotite formed with anhydrite, magnetite, and quartz. However, it cannot be ruled out that these minerals formed after the biotite because of a later overprint of the EB vein. B. High-magnification image showing the textural relationships in the EB vein. Plane-polarized light image. C. Corresponding crossed-polarized light image. D. Optical cathodoluminescence image showing the light-brown color of the anhydrite during electron bombardment. Quartz in the vein exhibits a dark-blue emission. The cathodoluminescence signal is optically similar to quartz present in A veins, suggesting that the quartz formed at high temperatures. All images from sample BH-68-782. Abbreviations: Anh = anhydrite, Bt = biotite, Kfsp = K-feldspar, Mag = magnetite, Qz = quartz.

biotite grains (Fig. 5A-D) or encloses small clasts of biotite (Fig. 5D). The textural relationships are inconsistent with the chalcopyrite being formed together with the biotite in the EB veins. No intergrowths of sulfide minerals with biotite, or the early high-temperature quartz present in some of the EB veins, were observed.

In some cases, biotite in contact with chalcopyrite in overprinted EB veins is largely unaltered (Fig. 5A), and only rare chlorite is present along the contacts and is only visible at high magnification. This may suggest that chalcopyrite deposition along the fractures reopening earlier EB veins took place largely at the conditions of biotite stability. In other cases, biotite is chloritized along contacts with crosscutting chalcopyrite and pyrite veins, providing unequivocal evidence that chlorite stability frequently prevailed during sulfide deposition (Fig. 5B-D).

Discussion and Conclusions

The study at Kuh-e Janja demonstrates that EB veins at this deposit are texturally early. The veins consisting primarily of biotite are crosscut by all younger vein generations recognized. This is consistent with other studies on porphyry deposits (Meyer, 1965; Brimhall, 1977; Gustafson and Quiroga, 1995; Atkinson et al., 1996; Rusk et al., 2008; Proffett, 2009; Redmond and Einaudi, 2010; Cernuschi et al., 2018, 2023; Ouyang et al., 2021), demonstrating that biotite-rich veins and alteration envelopes are early and were formed at high

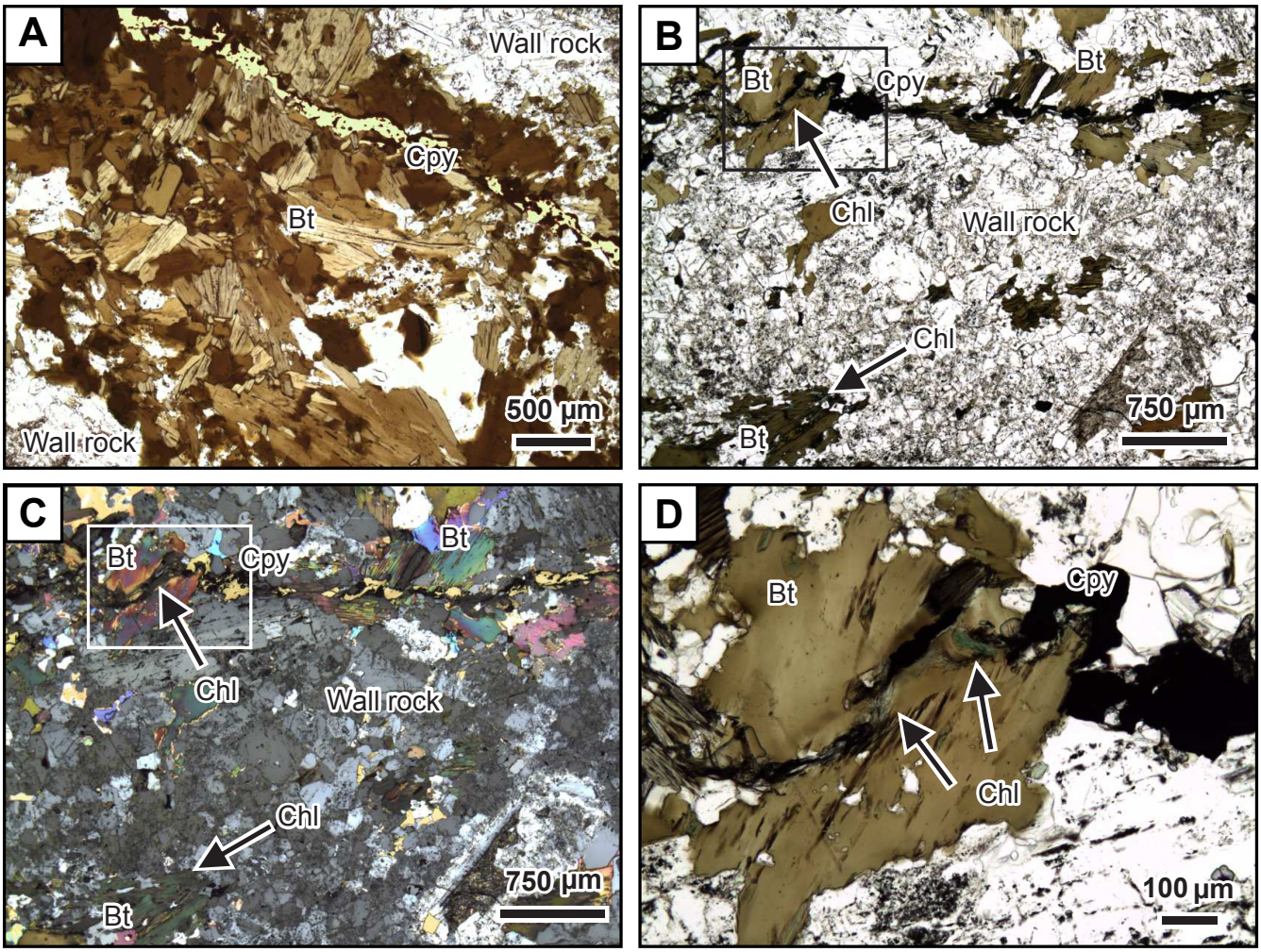

Fig. 5. Textural relationships in early biotite (EB) veins at the Kuh-e Janja Cu-Au porphyry deposit. A. EB vein that is crosscut by a hairline fracture that is filled by chalcopyrite. The hairline fracture is at a low angle to the EB vein and dissects some of the large biotite flakes. Microscopically, the biotite appears largely unaltered in contact with the chalcopyrite. At high magnification, however, minor chlorite alteration of biotite can be observed along the hairline fracture. Plane-polarized and reflected light. Sample BH68-787. B. Biotite that is crosscut by a hairline fracture filled with chalcopyrite. The biotite in the upper part of the photomicrograph forms part of an early dark micaceous alteration halo. Biotite in the lower part of the photomicrograph is located in the wall rock outside the alteration halo. Biotite in contact with the chalcopyrite as well as biotite in the wall rock has been partially replaced by chlorite. The rectangle shows the location of the high-magnification image in D. Plane-polarized light. Sample BH-68-785. C. Same field of view in crossed-polarized and reflected light showing the distribution of chalcopyrite along the hairline fracture crosscutting the earlier biotite. The rectangle shows the location of the high-magnification image in D. D. High-magnification image showing the partial replacement of biotite by chlorite. Chloritization of the biotite occurred along the hairline fracture that is partially filled with chalcopyrite. Sample BH-68-785. Abbreviations: Bt = biotite, Chl = chlorite, Cpy = chalcopyrite.

temperatures. Quartz solubility modeling by Monecke et al. (2018, 2019) showed that the apparent lack of quartz in the high-temperature EB veins can be related to their formation during quasi-isobaric cooling of single-phase magmatic-hydrothermal fluids at temperatures as high as ~500° to 650°C and pressures of up to 900 bar.

At the high formation temperatures of the EB veins, the host rocks exhibit ductile behavior. Early fluid flow through the ductile rock occurs through permeability created when the fluid pressures exceed the criterion for rock failure, which is above lithostatic for ductile rock. Numerical simulations by Weis et al. (2012) demonstrate that the magmatic-hydrothermal fluids responsible for the potassic alteration in the core of porphyry deposits move through the ductile rocks as plumes of rapid overpressure-permeability waves. It is envisaged here that these waves of high-temperature magmatic-hydrothermal fluids moving through the ductile host rock resulted in the formation of the EB veins and the later quartz-bearing A veins that are also associated with potassic alteration of the host rocks.

In many cases, early EB veins at Kuh-e Janja were overprinted during the later stages of porphyry vein formation

with later quartz or other gangue minerals occurring in the vein center or along the vein margins. Based on the microtextural observation, it is unclear whether the small amounts of high-temperature anhydrite and quartz present in some EB veins were coprecipitated with the biotite or introduced during reopening by later A veins. Anhydrite and quartz in A veins show identical petrographic characteristics and CL emission colors. In some cases, the EB veins are crosscut or reopened by AB veins, which are characterized by euhedral quartz crystals oriented perpendicular to vein walls or occur within vugs. Monecke et al. (2018) demonstrated that the euhedral quartz in AB veins forms close to the ductile-brittle transition at <500°C that is marked by significant pressure fluctuations due to cycling between lithostatic and hydrostatic conditions (Gustafson and Hunt, 1975).

Most EB veins at Kuh-e Janja do not contain chalcopyrite or pyrite, and this vein type is not abundant in ore zones. Representative hand specimens of biotite-rich veins hosting sulfide minerals were investigated microscopically in this contribution to unravel paragenetic relationships. In EB veins investigated petrographically, there are cases that show conclusive evidence that chalcopyrite and pyrite are texturally late and have not formed in association with biotite or high-temperature quartz that may be part of the EB veins or introduced during reopening of the EB veins during A or AB vein formation. The sulfide minerals are not intergrown with biotite. The high-temperature quartz does not contain encapsulated sulfide inclusions along growth zones. Chalcopyrite and pyrite appear to be paragenetically late, as microfractures containing them crosscut EB veins and the halos around them. At Kuh-e Janja, these microfractures are interpreted to be C veins. EB veins are refractured or crosscut by the C veins at low angles as the later fluid flow exploited preexisting structural weaknesses.

In many cases, hairline fractures coated with chalcopyrite and pyrite are associated with chlorite alteration of igneous or earlier formed hydrothermal biotite. In other cases, sulfide minerals are in contact with biotite, and no chlorite is observed with the optical microscope. Phase relationships in the K_2O-Al_2O_3-SiO_2-H_2O-KCl-HCl system at temperatures below the ductile-brittle transition at 400° to 450°C suggest that biotite stability is primarily controlled by acidity, with biotite being converted to chlorite only under moderate to acidic conditions (Fig. 6; Seedorff et al., 2005). With further decreases in temperature, chlorite stability expands (Fig. 6). The phase relationships may explain why chlorite alteration is limited at Kuh-e Janja. The relative mafic nature of the host rocks may have resulted in effective buffering of the acidity of the magmatic-hydrothermal fluids causing sulfide formation. The apparent absence of chlorite in some sulfide-bearing EB veins and the lack of pronounced chlorite alteration halos around some C veins are not reliable constraints on paragenesis. Moreover, it is important to note that pale-green to brown chlorite in alteration halos can be macroscopically mistaken for biotite (Reynolds and Beane, 1985).

The case study at Kuh-e Janja highlights that correct identification of paragenetic relationships in porphyry veins can be misleading at the hand-specimen scale. Overprinting of the earlier veins results in textural relationships that are complex even at the microscopic scale. Previous studies establishing the timing of hypogene Cu mineralization in porphyry deposits based on macroscopic observations should, therefore, be viewed with skepticism.

The findings at Kuh-e Janja add to the growing evidence from microscopic studies that Cu mineralization in at least some Cu-Mo and Cu-Au porphyry deposits is introduced late in the evolution of the magmatic-hydrothermal systems during C vein formation at temperatures below the ductile-brittle transition (Hedenquist et al., 1998; Landtwing et al., 2010; Bennett et al., 2014; Stefanova et al., 2014; Monecke et al., 2018, 2023; Sun et al., 2021; Tsuruoka et al., 2021; Schirra et al., 2022). At these temperatures the host rocks are brittle, allowing ore deposition along microfractures at hydrostatic pressures (Weis et al., 2012). The Bingham Canyon deposit in Utah is a prominent example of a Cu-Au porphyry deposit in which microscopic studies suggest that the hypogene Cu mineralization has been introduced at relatively low temperatures (Landtwing et al., 2010; Bennett et al., 2014; Monecke et al., 2018). At Bingham Canyon, Landtwing et al. (2010) showed that the deposition of chalcopyrite and bornite was associated with the dissolution of earlier-formed quartz. Monecke et al. (2018, 2019) demonstrated that late hypogene Cu mineralization occurs under conditions of retrograde quartz solubility at <450°C, explaining why the sulfide-bearing C veins in porphyry deposits do not typically contain quartz as a gangue mineral. Microtextural observations similar to those at Bingham Canyon have been reported from many porphyry

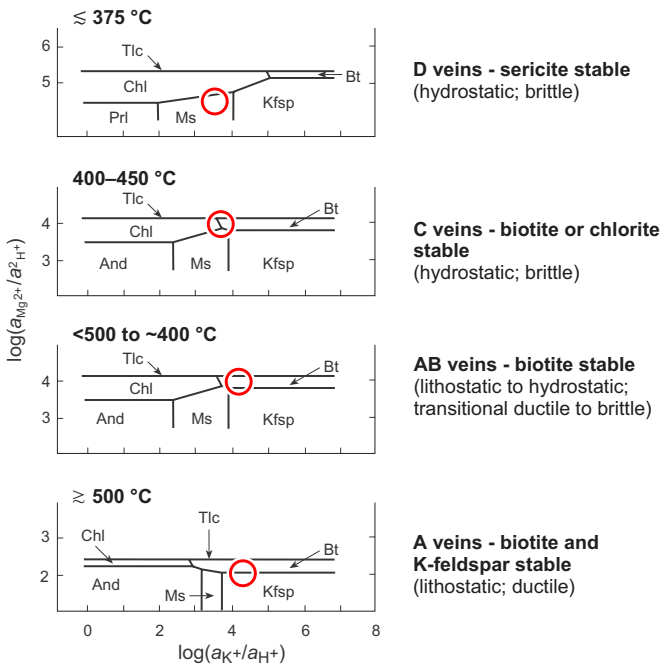

Fig. 6. Phase diagram for the system K_2O-Al_2O_3-SiO_2-H_2O-KCl-HCl depicting the stability of biotite and chlorite at the temperatures of formation of the different vein types in porphyry deposits. The diagram shows that biotite can be stable in wall-rock-buffered magmatic hydrothermal fluids at <450°C when C veins are formed. Chlorite stability expands toward lower temperatures. Phase diagram modified from Seedorff et al. (2005). Conditions of vein formation from Monecke et al. (2018). Abbreviations: And = andalusite, Bt = biotite, Chl = chlorite, Kfsp = K-feldspar, Ms = muscovite, Prl = pyrophyllite, Tlc = talc.

deposits, including Batu Hijau in Indonesia (Schirra et al., 2022), Elatsite in Bulgaria (Stefanova et al., 2014), Erdenetiin Ovoo in Mongolia (Monecke et al., 2023), Far Southeast in the Philippines (Hedenquist et al., 1998; Bennett et al., 2014; Calder et al., 2022), Santa Rita in New Mexico (Tsuruoka et al., 2021), and Yulong in China (Sun et al., 2021).

Acknowledgments

We gratefully acknowledge the Iran Minerals Production and Supply Company for providing site access and allowing us to use exploration data and core logs. We thank Sebastian Dettmar for thin-section preparation. Shahram Adib and Soheil Ghaffarzadeh are acknowledged for their assistance during this research. Funding was provided by the University of Tehran. Additional support was provided by the Center to Advance the Science of Exploration to Reclamation in Mining (CASERM), which is an industry-university collaborative research center between Colorado School of Mines and Virginia Tech under the National Science Foundation (NSF) awards 2310920 and 2310948. We thank Michael Calder and Mark Reed for reviewing the manuscript. Andreas Audétat is acknowledged for editorial handling.

REFERENCES

Angiboust, S., Agard, P., De Hoog, J.C.M., Omrani, J., and Plunder, A., 2013, Insights on deep, accretionary subduction processes from the Sistan ophiolitic "mélange" (Eastern Iran): Lithos, v. 156–159, p. 139–158.

Arancibia, O.N., and Clark, A.H., 1996, Early magnetite-amphibole-plagioclase alteration-mineralization in the Island Copper porphyry copper-gold-molybdenum deposit, British Columbia: Economic Geology, v. 91, p. 402–438.

Atkinson, W.W., Jr., Souviron, A., Vehrs, T.I., and Faunes G., A., 1996, Geology and mineral zoning of the Los Pelambres porphyry copper deposit, Chile: Society of Economic Geologists, Special Publication 5, p. 131–155.

Bennett, M., Monecke, T., Reynolds, T.J., Ricks, J., and Muntean, J., 2014, Cathodoluminescence and fluid inclusion characteristics of porphyry vein quartz [ext. abs.]: U.S. Geological Survey and Colorado State University, Pan-American Current Research on Fluid Inclusions Conference, 12th, Denver, Colorado, 2014, Program and Abstracts, p. 61–62.

Bonnet, G., Agard, P., Angiboust, S., Monié, P., Jentzer, M., Omrani, J., Whitechurch, H., and Fournier, M., 2018, Tectonic slicing and mixing processes along the subduction interface: The Sistan example (Eastern Iran): Lithos, v. 310–311, p. 269–287.

Boomeri, M., Moradi, R., Stein, H., and Bagheri, S., 2019, Geology, Re-Os age, S and O isotopic composition of the Lar porphyry Cu-Mo deposit, southeast Iran: Ore Geology Reviews, v. 104, p. 477–494.

Boomeri, M., Moradi, R., and Bagheri, S., 2020, Petrology and origin of the Lar igneous complex of the Sistan suture zone, Iran: Geologos, v. 26, p. 51–64.

Brimhall, G.H., Jr., 1977, Early fracture-controlled disseminated mineralization at Butte, Montana: Economic Geology, v. 72, p. 37–59.

Calder, M.F., Chang, Z., Arribas, A., Gaibor, A., Dunkley, P., Pastoral, J., Kouzmanov, K., Spandler, C., and Hedenquist, J.W., 2022, High-grade copper and gold deposited during postpotassic chlorite-white mica-albite stage in the Far Southeast porphyry deposit, Philippines: Economic Geology, v. 117, p. 1573–1596.

Camp, V.E., and Griffis, R.J., 1982, Character, genesis and tectonic setting of igneous rocks in the Sistan suture zone, eastern Iran: Lithos, v. 15, p. 221–239.

Cernuschi, F., Dilles, J.H., Grocke, S.B., Valley, J.W., Kitajima, K., and Tepley, F.J., III, 2018, Rapid formation of porphyry copper deposits evidenced by diffusion of oxygen and titanium in quartz: Geology, v. 46, p. 611–614.

Cernuschi, F., Dilles, J.H., Osorio, J., Proffett, J.M., and Kouzmanov, K., 2023, A reevaluation of the timing and temperature of copper and molybdenum precipitation in porphyry deposits: Economic Geology, v. 118, p. 931–965.

Chang, J., Li, J.W., Selby, D., Liu, J.C., and Deng, X.D., 2017, Geological and chronological constraints on the long-lived Eocene Yulong porphyry Cu-Mo deposit, eastern Tibet: Implications for the lifespan of giant porphyry Cu deposits: Economic Geology, v. 112, p. 1719–1746.

Clark, A.H., 1993, Are outsize porphyry copper deposits either anatomically or environmentally distinctive?: Society of Economic Geologists, Special Publication 2, p. 213–283.

Elyaspour, N., 2010, Economic geology and ore mineralization in Sefidabeh area (Kuh-e Janja), east of Iran: M.S. thesis, Zahedan, Iran, University of Sistan and Baluchestan, 282 p.

Fotoohi Rad, G.R., Droop, G.T.R., Amini, S., and Moazzen, M., 2005, Eclogites and blueschists of the Sistan suture zone, eastern Iran: A comparison of P-T histories from a subduction mélange: Lithos, v. 84, p. 1–24.

Gregory, M.J., 2017, A fluid inclusion and stable isotope study of the Pebble porphyry copper-gold-molybdenum deposit, Alaska: Ore Geology Reviews, v. 80, p. 1279–1303.

Gustafson, L.B., and Hunt, J.P., 1975, The porphyry copper deposit at El Salvador, Chile: Economic Geology, v. 70, p. 857–912.

Gustafson, L.B., and Quiroga G., J., 1995, Patterns of mineralization and alteration below the porphyry copper orebody at El Salvador, Chile: Economic Geology, v. 90, p. 2–16.

Hedenquist, J.W., Arribas, A., Jr., and Reynolds, T.J., 1998, Evolution of an intrusion-centered hydrothermal system: Far Southeast-Lepanto porphyry and epithermal Cu-Au deposits, Philippines: Economic Geology, v. 93, p. 373–404.

Landtwing, M.R., Furrer, C., Redmond, P.B., Pettke, T., Guillong, M., and Heinrich, C.A., 2010, The Bingham Canyon porphyry Cu-Mo-Au deposit. III. Zoned copper-gold ore deposition by magmatic vapor expansion: Economic Geology, v. 105, p. 91–118.

Lowell, J.D., and Guilbert, J.M., 1970, Lateral and vertical alteration-mineralization zoning in porphyry ore deposits: Economic Geology, v. 65, p. 373–408.

Maydagán, L., Franchini, M., Rusk, B., Lentz, D.R., McFarlane, C., Impiccini, A., Ríos, F.J., and Rey, R., 2015, Porphyry to epithermal transition in the Altar Cu-(Au-Mo) deposit, Argentina, studied by cathodoluminescence, LA-ICP-MS, and fluid inclusion analysis: Economic Geology, v. 110, p. 889–923.

Meyer, C., 1965, An early potassic type of wall-rock alteration at Butte, Montana: American Mineralogist, v. 50, p. 1717–1722.

Monecke, T., Monecke, J., Reynolds, T.J., Tsuruoka, S., Bennett, M.M., Skewes, W.B., and Palin, R.M., 2018, Quartz solubility in the H_2O-NaCl system: A framework for understanding vein formation in porphyry copper deposits: Economic Geology, v. 113, p. 1007–1046.

Monecke, T., Monecke, J., and Reynolds, T.J., 2019, The influence of CO_2 on the solubility of quartz in single-phase hydrothermal fluids: Implications to the formation of stockwork veins in porphyry copper deposits: Economic Geology, v. 114, p. 1195–1206.

Monecke, T., Reynolds, T.J., Gonchig, T., and Batbayar, N., 2023, Evolution of the magmatic-hydrothermal system at the Erdenetiin Ovoo porphyry Cu-Mo deposit, Mongolia: Constraints on the relative timing of alteration and mineralization: Mineralium Deposita, v. 59, p. 907–929.

Muntean, J.L., and Einaudi, M.T., 2000, Porphyry gold deposits of the Refugio district, Maricunga belt, northern Chile: Economic Geology, v. 95, p. 1445–1472.

Neuser, R.D., 1995, A new high-intensity cathodoluminescence microscope and its application to weakly luminescing minerals: Bochumer Geologische und Geotechnische Arbeiten, v. 44, p. 116–118.

Nielsen, R.L., 1968, Hypogene texture and mineral zoning in a copper-bearing granodiorite porphyry stock, Santa Rita, New Mexico: Economic Geology, v. 63, p. 37–50.

Ouyang, H., Mao, J., Hu, R., Caulfield, J., and Zhou, Z., 2021, Controls on the metal endowment of porphyry Mo deposits: Insights from the Luming porphyry Mo deposit, northeastern China: Economic Geology, v. 116, p. 1711–1735.

Proffett, J.M., 2009, High Cu grades in porphyry Cu deposits and their relationship to emplacement depth of magmatic sources: Geology, v. 37, p. 675–678.

Redmond, P.B., and Einaudi, M.T., 2010, The Bingham Canyon porphyry Cu-Mo-Au deposit. I. Sequence of intrusions, vein formation, and sulfide deposition: Economic Geology, v. 105, p. 43–68.

Rees, C., Riedell, K.B., Proffett, J.M., Macpherson, J., and Robertson, S., 2015, The Red Chris porphyry copper-gold deposit, northern British Columbia, Canada: Igneous phases, alteration, and controls of mineralization: Economic Geology, v. 110, p. 857–888.

Reynolds, T.J., and Beane, R.E., 1985, Evolution of hydrothermal fluid characteristics at the Santa Rita, New Mexico, porphyry copper deposit: Economic Geology, v. 80, p. 1328–1347.
Rusk, B.G., Reed, M.H., and Dilles, J.H., 2008, Fluid inclusion evidence for magmatic-hydrothermal fluid evolution in the porphyry copper-molybdenum deposit at Butte, Montana: Economic Geology, v. 103, p. 307–334.
Saccani, E., Delavari, M., Beccaluva, L., and Amini, S., 2010, Petrological and geochemical constraints on the origin of the Nehbandan ophiolitic complex (eastern Iran): Implication for the evolution of the Sistan Ocean: Lithos, v. 117, p. 209–228.
Schirra, M., Laurent, O., Zwyer, T., Driesner, T., and Heinrich, C.A., 2022, Fluid evolution at the Batu Hijau porphyry Cu-Au deposit, Indonesia: Hypogene sulfide precipitation from a single-phase aqueous magmatic fluid during chlorite–white-mica alteration: Economic Geology, v. 117, p. 979–1012.
Seedorff, E., Dilles, J.H., Proffett, J.M., Jr., Einaudi, M.T., Zurcher, L., Stavast, W.J.A., Johnson, D.A., and Barton, M.D., 2005, Porphyry deposits: Characteristics and origin of hypogene features: Economic Geology 100th Anniversary Volume, p. 251–298.
Sillitoe, R.H., 2010, Porphyry copper systems: Economic Geology, v. 105, p. 3–41.
Soleymani, M., Niroomand, S., Rajabi, A., and Lentz, D.R., 2020, Geological, geochemical and mineralogical investigation of Janja intrusion related and skarn (Au-Ag-Cu-Pb-Zn) deposit (Southeast of Nehbandan, Iran) [abs.]: GSA 2020 Connects Online, Virtual, Geological Society of America Abstracts with Programs, v. 52, paper 1-19.
Stefanova, E., Driesner, T., Zajacz, Z., Heinrich, C.A., Petrov, P., and Vasilev, Z., 2014, Melt and fluid inclusions in hydrothermal veins: The magmatic to hydrothermal evolution of the Elatsite porphyry Cu-Au deposit, Bulgaria: Economic Geology, v. 109, p. 1359–1381.
Stöcklin, J., 1968, Structural history and tectonics of Iran: A review: The American Association of Petroleum Geologists Bulletin, v. 52, p. 1229–1258.
Sun, M., Monecke, T., Reynolds, T.J., and Yang, Z., 2021, Understanding the evolution of magmatic-hydrothermal systems based on microtextural relationships, fluid inclusion petrography, and quartz solubility constraints: Insights into the formation of the Yulong Cu-Mo porphyry deposit, eastern Tibetan Plateau, China: Mineralium Deposita, v. 56, p. 823–842.
Tirrul, R., Bell, I.R., Griffis, R.J., and Camp, V.E., 1983, The Sistan suture zone of eastern Iran: Geological Society of America Bulletin, v. 94, p. 134–150.
Titley, S.R., and Beane, R.E., 1981, Porphyry copper deposits: Economic Geology 75th Anniversary Volume, p. 214–269.
Tsuruoka, S., Monecke, T., and Reynolds, T.J., 2021, Evolution of the magmatic-hydrothermal system at the Santa Rita porphyry Cu deposit, New Mexico, USA: Importance of intermediate-density fluids in ore formation: Economic Geology, v. 116, p. 1267–1284.
Weis, P., Driesner, T., and Heinrich, C.A., 2012, Porphyry-copper ore shells form at stable pressure-temperature fronts within dynamic fluid plumes: Science, v. 338, p. 1613–1616.

Majid Soleymani is an economic geologist who has expertise in studying porphyry copper, epithermal gold, and iron oxide-apatite deposits. He obtained his B.Sc. degree in geology from the University of Tehran in 2019 and successfully completed his M.Sc. in economic geology in 2023. Throughout this time, he worked as a geologist for the Iran's Exploration Services Company. Currently, Majid is a Ph.D. student of economic geology and a lecturer at the University of Tehran, where he studies the metallogeny of porphyry copper deposits in southeastern Iran.